In vitro 3-D Measurement of Tissue Viscoelasticity by Ultrasound

Tsuyoshi Shiina*,

Invited Paper

ABSTRACT

It is well known that elasticity and viscosity of tissues reflect pathological change of tissues caused by diseases such as cancer. We recently developed commercial-based ultrasound equipment for tissue elasticity imaging. In order to evaluate the stages of a progressive disease and to discriminate benign from malignant tumors, it is important to clarify the relationship between the elasticity of tissues and their pathological meanings. However, no database for such a relationship has been yet established. With the aim of constructing such database, we tried to develop the three-dimensional tissue viscoelasticity microscope, which can quantitatively measure 3D distribution of parameters on tissue elasticity and viscosity. Results of experiments using a phantom model made of konnyaku and acrylamide confirmed that the system could reveal the difference of elasticity and viscosity of tissues.

Keywords: Tissue characterization; Ultrasound microscope; Elastic modulus; Viscoelasticity

1. INTRODUCTION

Ultrasonic tissue elasticity imaging can provide us novel diagnostic information based on tissue hardness and consequently it is expected to detect tumor with high contrast and also discriminate benign and malignant disease.

We recently developed commercial-based equipment for tissue elasticity imaging which is used for diagnosing diseases such as breast cancer. By clinical evaluation of the equipment, it was revealed that elasticity image enables examiner to attain high precision of diagnosis with simpler criterion based on elasticity image than conventional ultrasonogram. In order to evaluate the stages of a progressive disease and to discriminate benign from malignant tumors, it is important to clarify the relationship between the elasticity of tissues and their pathological meanings. However, no database for such a relationship has been yet established.

There is some pioneer research on the measurement of the elastic modulus of tissues such as excised breast tissue. [7] And some approaches to the microscopic measurement of tissue elasticity have been proposed. [8] These methods are aimed at attaining higher spatial resolution with high frequency ultrasound, consequently, thin slices of tissue must be used to prevent the attenuation of ultrasound.

However, such thin slices are two-dimensional (2D) distributions, and the real mechanical properties of tissue are apt to change when the tissue is sliced thinly since the tissue microstructure is destroyed. To evaluate the mechanical properties of tissues under similar conditions to clinical use, it is important to measure the three-dimensional (3D) distribution of mechanical properties by using a relatively thick specimen to preserve the microstructure of tissues.

On the other hand, in the elasticity imaging based on the static method, tissue is deformed by compression and relaxation similar to palpation. Under such situations, most soft tissues behave as viscoelastic bodies. It is empirically well known that the stress-strain relationship of soft tissue exhibits a hysteresis loop in both processes of loading and unloading.

Since these viscoelastic properties reflect the tissue type, in addition to the tissue elasticity, detecting these parameters may improve the accuracy of the diagnosis. We previously introduced quantitative parameters to evaluate these viscoelastic properties of soft tissues and developed the ultrasonic procedures to detect these parameters. [9, 10]

From the above viewpoint, we are investigating the development of a 3D tissue viscoelasticity microscope for accumulating quantitative data on the mechanical properties of tissues. In this study, the primary system was constructed and its basic performance was evaluated using a tissue phantom. This paper is constructed as follows. In Section 2, the measurement of the parameters of tissue elasticity and viscosity and the measurement system are described, and in Section 3, spatial and contrast resolution are discussed on the basic of simulation and theoretical analysis. To validate the feasibility of the system, a phantom experiment was conducted as described in Section 4. Finally, in Section 5, we conclude our paper.

2. PARAMETERS ON TISSUE ELASTICITY AND VISCOSITY

Among the various approaches to elasticity imaging, the static method has the advantages that the system is simple since no other additional devices

Manuscript received on April 15, 2008 ; revised on May 16, 2008.

* Corresponding author.

T. Shiina is with Graduate School of Systems and Information Engineering, University of Tsukuba, Tsukuba Japan

E-mail addresses: shiina@hs.med.kyoto-u.ac.jp (T. Shiina)

than a probe is required, and it is easy to reconstruct elasticity images with high spatial resolution since strain is basically obtained by comparing RF signals of two frames. In addition, the data acquisition time is of the same order as that of conventional ultrasonography, which is suited to three-dimensional measurement. Therefore, a practical system for clinical use, based on static methods, has recently been developed by us in cooperation with medical-equipment makers. [5, 6] Considering the process of elasticity imaging for clinical diagnosis, the microscopic measurement proposed in this study is also based on static methods.

In terms of the elastic properties of tissues, Young's modulus is defined as the slope of the stress-strain curve as follows:

$$E(\varepsilon) = \frac{\partial \sigma(\varepsilon)}{\partial \varepsilon} \tag{1}$$

where E is Young's modulus, and σ and ε indicate axial stress and axial strain, respectively.

It is well known that the stress-strain relationship of most soft tissue exhibits the exponential property, [15, 16] Young's modulus-strain curve is also shown by [9, 10]

$$E(\varepsilon) = E_0 \cdot e^{\beta \cdot \varepsilon} \tag{2}$$

Parameter E_0 corresponds to Young's modulus of a linear elastic body under slight deformation, and parameter β quantifies the intensity of the elastic nonlinearity of soft tissue. By taking the logarithm of both sides of eq.(2), the exponential curve is converted to a linear profile, as shown by eq.(3). Therefore, parameters E_0 and β can be obtained by applying the least-squares method to the profile.

$$\log E(\varepsilon) = \log E_0 + \beta \cdot \varepsilon \tag{3}$$

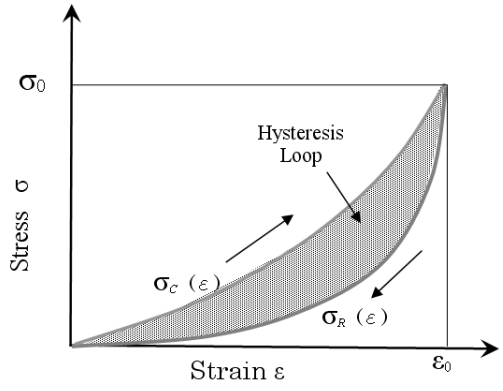

Fig.1: *Typical hysteresis loop of stress-strain curves in soft tissue.*

In general, the stress-strain curve in the relaxation process falls below that in the compression process because of strain energy dissipation, as illustrated in Fig. 1. The area of the hysteresis loop,H , reflects each tissue type. For example, the value of H of a ligament is relatively small, while that of smooth muscle is fairly large. To discriminate between normal and pathological tissue, such as carcinoma, it is expected that the area of the hysteresis loop will play an important role in actual clinical diagnosis based on tissue viscoelasticity.

Since the area of the hysteresis loop is dependent on strain at the turn-around point, at which the compression process switches to the unloading process, for quantitative assessment of the hysteresis property, we introduced the following hysteresis parameter HP,

$$HP = \frac{\int_0^{\varepsilon_0} \sigma_c(\varepsilon) d\varepsilon - \int_0^{\varepsilon_0} \sigma_R d\varepsilon}{\int_0^{\varepsilon_0} \sigma_c d\varepsilon}, \tag{4}$$

where $\sigma_c(\varepsilon)$ and $\sigma_R(\varepsilon)$ are the stress-strain curves in the compression and relaxation processes, respectively. The parameter HP takes a value within 0 and 100%, and a large value of HP implies that viscosity is dominant. The processing details are described in the next section.

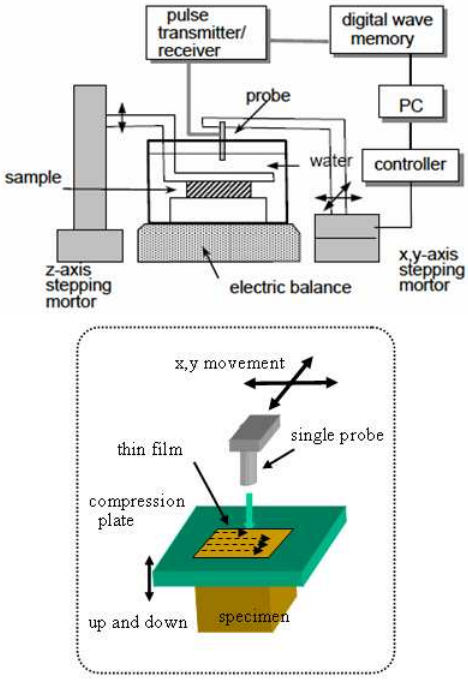

Fig.2: *Measurement system.*

For 3D microscopic measurement of tissue viscoelasticity, we constructed an experimental system, as shown in Fig.2. By considering the appropriate penetration depth and spatial resolution, a probe with a relatively low frequency, 20 MHz is used to image a thick specimen, for example, more than 5 mm. A specimen is placed in degassed water and compressed by a plate. A thin film is stretched on the hole which is opened at the center of the plate.

The water tank is placed on an electric balance to measure the pressure during compression. First, volumetric data of echo signals from the tissue specimen is obtained by scanning the probe in the horizontal direction or the xy plane.

Next, after the tissue specimen is compressed by the plate driven by a stepping motor, another set of volumetric data of echo signals is obtained by scanning the probe in the xy plane. At the same time, the applied pressure is also recorded by the electric balance.

To obtain the parameters E and HP, first, the three-dimensional distribution of axial strain under small deformation is obtained from echo signals in adjacent frames using the combined autocorrelation method (CAM) that we developed for clinical equipment for real-time tissue elasticity imaging [3,5,5], as shown in Fig.3.

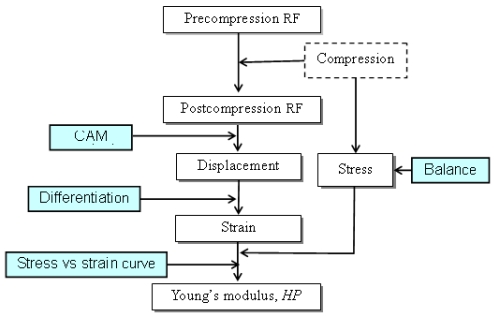

Fig.3: *Flowchart for data acquisition and image reconstruction.*

We assumed that stress distribution is uniform within the specimen and the surface pressure mechanically measured with the sensor was assigned as the internal stress value. This approximation is reasonable since the area of the compression plate is sufficiently large compared with the thickness of the specimen.

Next, Young's modulus-strain curve is profiled to obtain E_0 using eq.(3).

Finally, the stress-strain curve or hysteresis loop at each portion is obtained on the basis of the accumulated strain and the surface pressure during the compression and relaxation processes. Then HP is obtained using eq.(4).

3. ANALYSIS OF RESOLUTION

The resolution of the elastic modulus image is affected by many factors of the measurement system and signal processing, such as wavelength, beam width and window size of correlation calculation. Therefore, we evaluated the resolution of the elastic modulus by simulation using the 3D tissue model. A spherical inclusion was embedded in a plate 10.8 mm (H) × 14.8 mm (W) × 5.6 mm (D) with a hardness of Young's modulus of 10 kPa as shown in Fig. 4(a). Scatterers as echo sources with random scattering coefficients were distributed throughout the phantom.

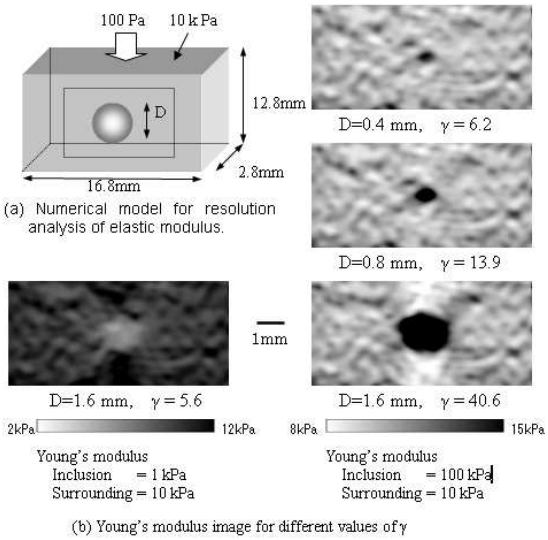

Fig.4: *Simulation analysis of spatial and contrast resolution*

The upper surface of the model was compressed with a pressure of 100 Pa to generate the mean strain of 1%. The deformation of tissue was calculated using the 3D finite element method. First, the three-dimensional displacement of each node induced by compression was calculated and the position of each scatterer after deformation was obtained by interpolation of the nodal position. Next, RF signals were generated by convolving the scatterer distribution with a three-dimensional point spread function (PSF). The PSF was obtained by simulating the acoustic field considering the attenuation properties of tissues.

Each parameter of the measurement system was set to approximately correspond to that in the experiment. For example, the center frequency was 20 MHz, pulse width was 0.108 mm and the interval of scan lines was 0.05 mm in both the lateral and elevational directions. Each frame was composed of 360 lines. The beam width at the focal point was 0.32 mm. The data was captured at the rate of 240 MHz and accuracy of 11 bits.

Many images of Young's modulus for different diameters and hardness of inclusions were prepared. To evaluate spatial and contrast resolutions, we employed parameter γ defined as

$$\gamma = \frac{\Delta E_{max}}{\sigma_{sur}}, \tag{5}$$

where ΔE_{max} represents the maximum difference between the Young's modulus around the inclusion and that of the surrounding region, and σ_{sur} is the standard deviation of Young's modulus of the surrounding

region. Generally, as γ increases, it becomes easy to recognize the inclusion. On the basis of perceptional examination of the obtained Young's modulus image, we set the threshold of γ as 2.5.

The image contrast between inclusion and surrounding tissue, CE, is defined by

$$C_E = \frac{E_{in} - E_{sur}}{E_{in} + E_{sur}}, \tag{6}$$

where E_{in} is Young's modulus of the inclusion and E_{sur} is that of the surrounding tissue.

For example, Fig. 4(b) shows Young's modulus image for four cases with different values of γ. The inclusion is clearly imaged in the case of hard inclusion D=1.6 mm diameter with γ=40.6, while it is possible to recognize the inclusion in the case of hard inclusion D=0.4 mm diameter with γ=6.2. In the case of soft inclusion, it becomes more difficult to recognize the inclusion compared with hard inclusion as shown at the lower left of Fig. 4(b)

The relationship between spatial and contrast resolutions was examined for different values of Young's modulus and inclusion diameters. As a results, for example, in the case of C_E =50%, which corresponds to E_{in} = 30 kPa and E_{sur}=10 kPa, the spatial resolution is about 0.8 mm. And in the case of C_E =82% (E_{in} = 100 kPa, E_{sur}=10 kPa) the spatial resolution is about 0.4 mm.

4. EXPERIMENT AND RESULTS

To validate the feasibility of the system, a phantom experiment was conducted. The phantom of the tissue specimen was made of gelatin and included a piece of boiled spaghetti with different sides (0.4, 0.6, 0.8mm). Young's modulus E_o of gelatin measured by a mechanical method is about 16 kPa for 10% strain as shown in Fig. 5, whereas that of the boiled spaghetti is about 139 kPa.

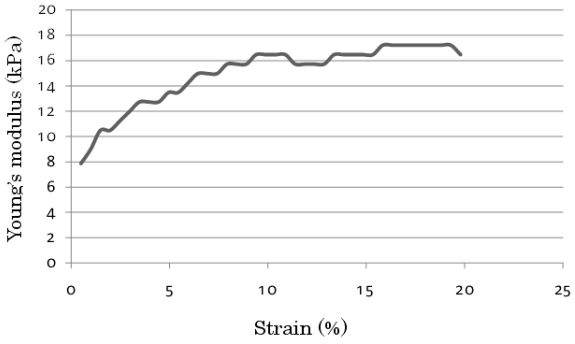

Fig.5: *Mechanically measured Young's modulus of gelatin.*

The phantom was scanned at intervals of 0.1mm in the lateral. Each set of frame data was captured at the rate of 250MHz and 11 bits. Figure 6 shows that the inclusion 0.8 and 0.6mm sides were clearly

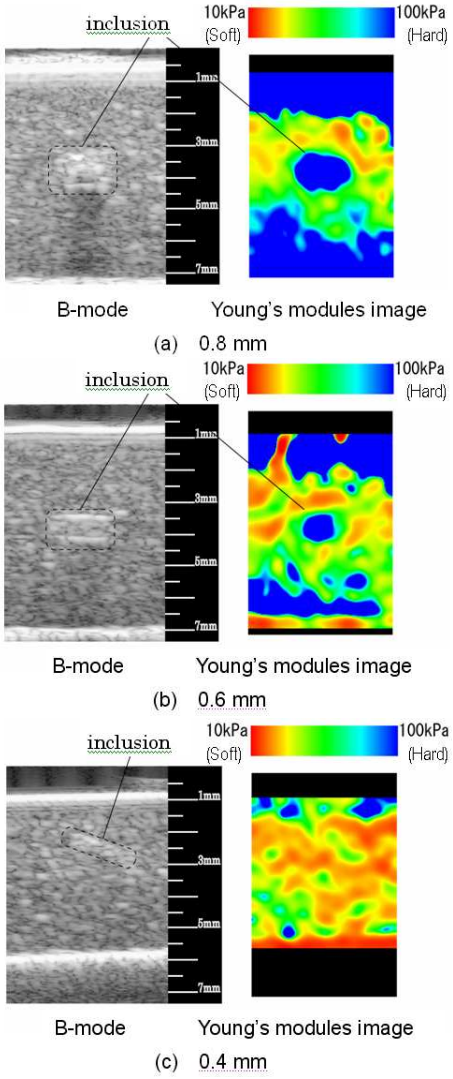

Fig.6: *Evaluation of spatial resolution of elastic modulus image reconstructed using the measurement system.*

imaged, although the image of the inclusion 0.4 mm side was somewhat unclear. It can be said that the spatial resolution is about 0.6 mm for this measurement system. In order to precisely evaluate spatial and contrast resolutions in comparison of the results of simulation analysis, a more appropriate phantom is required.

Next, tissue specimen was measured. The specimen was 4mm slice of pig liver. Figure 6 (a) shows a photograph of cross section and white spot near center is heat-denatured using nichrome wire. The specimen was scanned at intervals of 0.1mm in the lateral, x, and the elevational, y, direction. The scanned volume was 5 (lateral) $\times$ 5 (axial) $\times$ 2 (elevational) mm^3. The pulse motor for compression and relaxation of specimens was driven by 10 μm, which corresponds to an average deformation of 0.2%. Each set of frame data was captured at the rate of 250MHz and 11 bits.

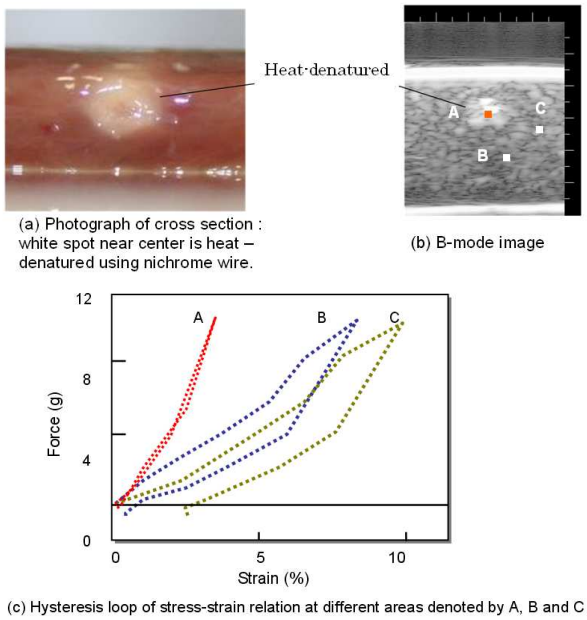

Fig.7: *Tissue specimen (4mm slice of pig liver)*

All frames were acquired under the equilibrium state. Figure 7(c) shows hysteresis loops of stress-strain relation which were mechanically measured at different areas denoted by A, B and C in Fig. 7(b). The area of the loop at A is extremely small compared with other points, which means heat-denatured area became reduced in the viscosity. The measured values of elastic modules E_0 and hysteresis parameter HP are summarized in table 1 which indicates the difference between raw and heat-denatured tissues.

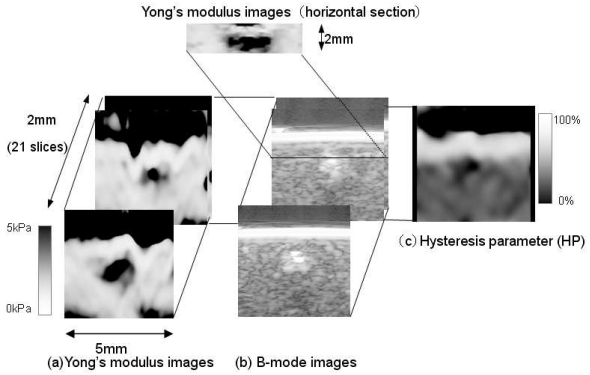

Fig.8: *A result of experiment (pig liver)*

Figure 8(a) shows the result of the measurement of the three-dimensional distribution of elastic modulus E_o. The inclusion is clearly imaged as a hard region and the value of the elastic modulus (Young's modulus) was coincident with that measured mechanically. It was validated that the system has sufficient spatial resolution to image a denatured area 1mm thick as well as B-mode imaging but has higher contrast.

Finally, Figure 8(c) shows a reconstructed image of hysteresis parameter HP. The inclusion is displayed as having a low value of HP which is coincident with the results of mechanical measurement.

Table 1: *Measured E_0 and HP for raw and heat-denatured tissue*

Location	Raw		Heat-denatured	
	E_0(kPa)	HP(%)	E_0(kPa)	HP(%)
1	2.9	57.2	7.4	50.0
2	2.6	55.1	17.5	50.1
3	3.7	62.6	12.8	49.0
average	3.1	58.3	12.6	49.7

5. CONCLUSION

We constructed the basic system of a three-dimensional tissue viscoelasticity microscope and verified its feasibility for measuring the three-dimensional distribution of the elastic modulus and hysteresis parameter as viscoelastic properties of tissue, even for relatively thick specimen.

The results of experiments using a phantom showed that three-dimensional distributions of the elastic modulus were obtained with reasonable resolution and precision using our basic system with a 20 MHz center frequency. The results of simulation analysis for spatial and contrast resolutions nearly coincided with those of the phantom experiment.

The reconstructed image of the hysteresis parameter showed some coincidence with the real distribution. However, the results revealed that there was still room for improvement in the precision of strain estimation.

In future work, we will continue the basic investigation to finalize the system to enable its use in accumulating the characteristics of tissue with respect to pathological results. Although the distribution of stress was assumed to be uniform in this study, we should calculate the stress distribution by the finite element method to confirm whether there is a significant difference in estimated parameters or not. Another important aspect is to determine the optimal specifications, for example, frequency, pulse waveform and material of compressing thin film, for a practical system.

6. ACKNOWLEDGMENT

This work was supported by Grants-in-Aid for Scientific Research from the Ministry of Education, Culture, Sports, Science and Technology, Japan and Nakatani Foundation of Electronic Measurement Technology Advancement.

References

[1] J. Ophir, I. Cespedes, H. Ponnekanti, Y. Yazdi, and X. Li: Elastography: Ultrason. Imag 13 (1991) 111.

[2] K. J. Parker, S. R. Huang, R. A. Musulin, and R. M. Lerner: Ultrason. Med Biol 16 (1990) 241.

[3] T. Shiina, N. Nitta, E. Ueno, and J. C. Bamber : Journal of Medical Ultrasonics 29 (2002) 119.

[4] J. Tang, H. Hasegawa, and H. Kanai : Jpn. J. Appl. Phys. 44 (2005) 4588.

[5] A. Itoh, E. Ueno, E. Tohno, H. Kamma, H. Takahashi, T. Shiina, M. Yamakawa, and T. Matsumura : Radiology, 231 (2006) 341.

[6] M. Yamakawa, N. Nitta, T. Shiina, T. Matsumura, S. Tamano, T. Mitake, and E. Ueno: Jpn. J. of Appl. Phys. 42 (2003) 3265.

[7] T. A. Krouskop, T. M. Wheeler, F. Kallel, B. S. Garra, and T. Hall: Ultrason. Imag. 20 (1998) 260.

[8] N. A. Cohn, S. Y. Emelianov, M. A. Lubinski, and M. O'Donnell : IEEE Trans. Ultrason. Ferroelect., Freq. Contr. 44 (1997) 1304.

[9] N. Nitta and T. Shiina: Jpn. J. Appl. Phys. 41 (2002) 3572

[10] N. Nitta, T. Shiina, and E. Ueno : Proc. of 2003 IEEE International Ultrasonics Symposium (2003) 1606.

[11] M. Yamakawa, T. Shiina Jpn.J.of Appl. Phys. 44 (2005) 4567.

[12] B. J. Fahey, K. R. Nightingale, D. L. Stutz and G.. E. Trahey: Ultrasound in Med. & Biol. 30 (2004) 321.

[13] M. Fatemi, L. E. Wold, A. Alizad, J. F. Greenleaf : IEEE UFFC Trans. 21(2002) 1.

[14] H. Hasegawa and H. Kanai : Jpn. J. Appl. Phys. 43 (2004) 3197.

[15] K. Hayashi: Baiomekanikusu (Biomechanics), Corona Publishing, Tokyo (2000) [in Japanese].

[16] Y. C. Fung: Biomechanics: Mechanical Properties of Living Tissues, 2nd ed. Springer-Verlag, New York (1993).

T. Shiina was born in Japan on May 5th, 1957. He was graduated from the faculty of Engineering and graduate school of Engineering, the University of Tokyo and received the BE, MS and PhD degrees in electronic engineering in 1982, 1984 and 1987, respectively, from the University of Tokyo. He also received Dr of Medical Science in 2007, from the University of Tsukuba.

From 1987 to 1992, he was Lecturer and Associate Professor at the Department of Electronic Engineering, Tokyo University of Agriculture and Technology. In 1992, he moved to the University of Tsukuba, as an Associate Professor of Institute of Information Sciences and Electronics. From 2001 to 2008, he has been a Professor of the University of Tsukuba. From 1995 to 1996, he was with the institute of Cancer Research and the Royal Marsden NHS Trust in UK as Visiting Professor. In 2008, he transferred to Kyoto University, as a Professor of Graduate School of Medicine, Human Health Sciences.

His current research interests include visualization technique of structural and functional bio-information, for example, ultrasonic elasticity imaging, 3D blood-flow measurement, and brain function imaging based on biological signal processing.

He was awarded the distinguished paper prize about his research on elasticity imaging and Novel Technology Prize for his major contribution in the field of medical ultrasound imaging by the Japan Society of Ultrasonics in Medicine, 2000 and 2003, 2008, respectively. In 2004, He developed the real-time tissue elasticity imaging system in corporative with HITACHI Medical Corporation.

Dr. Shiina performs editorial work of many academic journals such as Ultrasound in Medicine and Biology. He is Councilor of the Japan Society of Medical Electronics and Biological Engineering. He is also Executive Trustee of the Japan Society of Ultrasonics in Medicine (JSUM). He is the president of 2009 Annual Conference of JSUM to be held in Tokyo on May 22-24, 2009.